OCEANOGRAPHY

Accelerated freshening of Antarctic Bottom Water over the last decade in the Southern Indian Ocean

Viviane V. Menezes,[1]* Alison M. Macdonald,[1] Courtney Schatzman[2]

Southern Ocean abyssal waters, in contact with the atmosphere at their formation sites around Antarctica, not only bring signals of a changing climate with them as they move around the globe but also contribute to that change through heat uptake and sea level rise. A repeat hydrographic line in the Indian sector of the Southern Ocean, occupied three times in the last two decades (1994, 2007, and, most recently, 2016), reveals that Antarctic Bottom Water (AABW) continues to become fresher (0.004 ± 0.001 kg/g decade^{-1}), warmer (0.06° ± 0.01°C decade^{-1}), and less dense (0.011 ± 0.002 kg/m^3 decade^{-1}). The most recent observations in the Australian-Antarctic Basin show a particularly striking acceleration in AABW freshening between 2007 and 2016 (0.008 ± 0.001 kg/g decade^{-1}) compared to the 0.002 ± 0.001 kg/g decade^{-1} seen between 1994 and 2007. Freshening is, in part, responsible for an overall shift of the mean temperature-salinity curve toward lower densities. The marked freshening may be linked to an abrupt iceberg-glacier collision and calving event that occurred in 2010 on the George V/Adélie Land Coast, the main source region of bottom waters for the Australian-Antarctic Basin. Because AABW is a key component of the global overturning circulation, the persistent decrease in bottom water density and the associated increase in steric height that result from continued warming and freshening have important consequences beyond the Southern Indian Ocean.

INTRODUCTION

Antarctic Bottom Water (AABW) is changing (*1*–*15*). A key component of the ocean's overturning circulation, AABW brings dense, relatively oxygen- and nutrient-rich waters into the abyss of all the major ocean basins (*16*, *17*). Changes in the temperature and salinity characteristics of these waters can both directly and indirectly affect circulation, ocean heat content, sea level rise (*1*, *10*, *18*), and Earth's climate over decadal to millennial to glacial-interglacial time scales (*19*–*21*).

AABW is the common name for the bottom waters formed around the Antarctic continental margins. Four main formation regions have been identified: the Weddell Sea (60°W to 0°), the Cape Darnley polynya (65°E to 69°E) in the Enderby Basin, the George V/Adélie Land Coast (136°E to 154°E), and the Ross Sea (160°W to 180°W) (*5*, *16*, *22*). Several varieties of AABW exist, and their temperature and salinity characteristics depend on their formation region (*16*). For example, Ross Sea bottom waters are the warmest and saltiest AABW variety ($-0.6°C \leq \theta \leq -0.3°C$, $S_p > 34.72$, where θ is the potential temperature and S_p is the practical salinity), whereas Weddell Sea bottom waters are the coldest and freshest ($\theta < -1°C$, $S_p < 34.64$) (*16*).

Warming and freshening of bottom water throughout much of the Southern Hemisphere have been revealed by repeat hydrographic transects occupied in the 1990s and 2000s (*10*). At present, hydrography is the only available tool for observing the abyssal ocean (>3000 dbar) on basin scales (*23*). Here, we concentrate on repeat observations provided by the I08S (95°E) hydrographic line between 66.5°S and 28°S in the southeast Indian sector of the Southern Ocean (Fig. 1). The I08S line runs northward from the Antarctic Shelf, across the Princess Elizabeth Trough (PET), over the eastern side of the Kerguelen Plateau through the Australian-Antarctic Basin, and across the Southeast Indian Ridge to the South Australian Basin (SAB). This study includes the most recent observations obtained from the 2016 GO-SHIP (Global Ocean Ship-based Hydrographic Investigations Program) I08S expedition combined with data collected during the 2007 and 1994 occupations (table S1).

Much of the AABW in the Australian-Antarctic Basin and the PET is supplied by sources located to the east along the George V/Adélie Land Coast and the Ross Sea (*2*, *5*, *12*, *16*, *24*). Broadly speaking, AABW formed along the George V/Adélie Land Coast is cooler, fresher, and richer in oxygen than that formed in the Ross Sea (*2*, *12*, *25*). AABW formed in these regions is advected by a vigorous system of boundary currents that flow from the Pacific to the Indian Ocean, south of 60°S at neutral densities (γ^n) > 28.34 kg/m^3 (Fig. 1) (*5*, *12*, *16*, *26*, *27*). There is also a small contribution of slightly less dense AABW produced in the Weddell-Enderby Basin. These waters are transported eastward to the Australian-Antarctic Basin at $\gamma^n > 28.27$ kg/m^3 (*16*).

This study presents new evidence indicating that abyssal waters in the Australian-Antarctic Basin continue to become fresher, warmer, and less dense. The new observations also reveal a strikingly accelerated freshening of AABW between 2007 and 2016, which is significantly stronger than that found in the earlier period (1994–2007). We suggest that the strong decrease in AABW salinity in the Australian-Antarctic Basin observed between 2007 and 2016 may be linked to an abrupt iceberg-glacier collision-calving event that occurred in 2010.

RESULTS

Given the variety of source regions, it is hardly surprising that definitions of AABW have not always been consistent. However, generally speaking, AABW is defined either in terms of potential temperature or density (*5*, *6*, *9*, *10*, *12*, *16*, *27*). In keeping with the literature, here for the analysis in pressure space, AABW is defined as the waters with potential temperature lower than 0°C (*6*, *9*, *10*, *27*). In the PET, this includes some waters as shallow as 2000 dbar, whereas in the Australian-Antarctic Basin, these waters are deeper than 2500 dbar near the Kerguelen Plateau at 57°S and deeper than 3500 dbar at 52°S. North of this latitude, and particularly in the SAB, there are no waters this cold. When working in density space, we define AABW as waters with neutral

[1]Physical Oceanography Department, Woods Hole Oceanographic Institution, 266 Woods Hole Road MS#21, Woods Hole, MA 02543–11050, USA. [2]Oceanographic Data Facility, Scripps Institution of Oceanography, University of California, San Diego, 9500 Gilman Drive, La Jolla, CA 9209, USA.
*Corresponding author. Email: vmenezes@whoi.edu

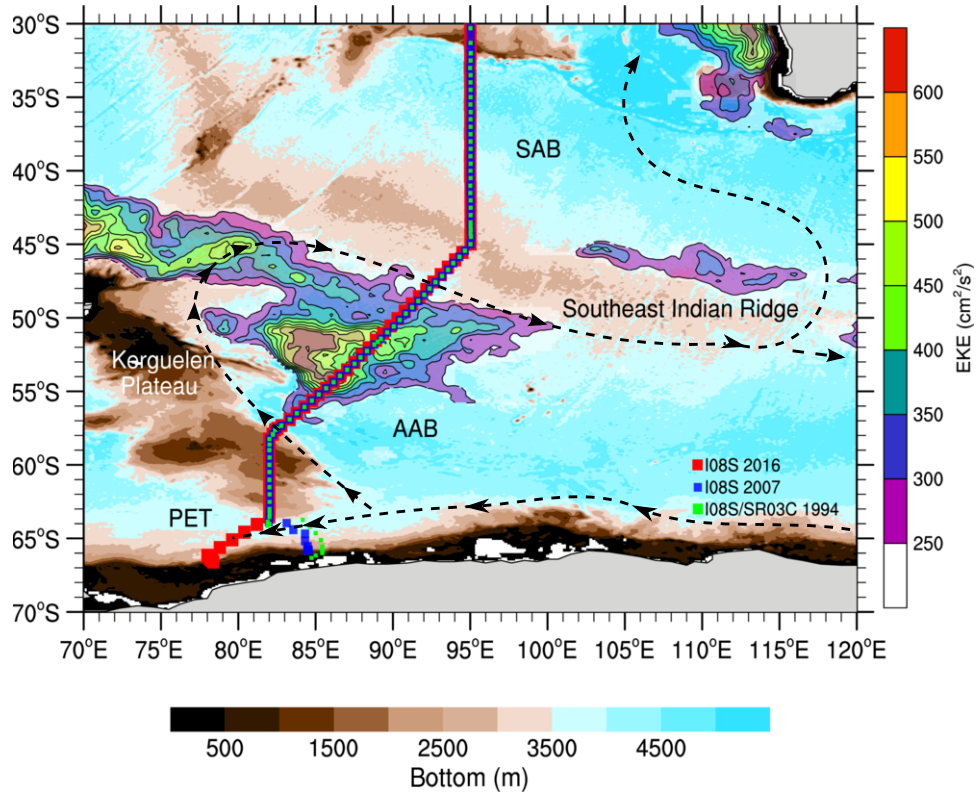

Fig. 1. Location of stations from the three I08S occupations in the southeastern Indian Ocean (filled squares), local bottom depths (blue to brown shading), and mean eddy kinetic energy field (rainbow map). The dashed line is a schematic view of AABW circulation based on the studies by Rintoul (*5*) and Orsi *et al*. (*16*). Bottom depths are 2-min bathymetry (*40*). Eddy kinetic energy (EKE) field is from 20 years of multisatellite altimetry data. Only EKE values larger than 250 cm^2/s^2 are plotted. South of 63°S, the 1994 I08S occupation is augmented by data from the Australian SR03C line. AAB, Australian-Antarctic Basin.

density (γ^n) greater than 28.27 kg/m^3 (*5*, *6*, *9*, *10*, *12*, *16*, *27*). Along the I08S line, both criteria produced similar results (not shown). Therefore, the patterns described here are independent of the particular criterion used to define AABW.

Here, all salinities are reported on the Thermodynamic Equation of SeaWater 2010 (TEOS-10) Absolute Salinity (S_a) scale that has units of gram per kilogram. Absolute Salinity may have values as much as 0.0247 greater than the practical salinity [Practical Salinity Scale 1978 (PSS-78)] in the open ocean (*28*). Although our AABW definition is based on potential temperature for the sake of consistency, temperatures are reported throughout this paper as conservative temperatures (Θ). The differences between potential (θ) and conservative (Θ) temperatures are very small (*28*). For the AABW salinity range, θ = 0°C is equivalent to Θ ≈ 0.001°C. Throughout this paper, the term "significant" implies a 95% confidence level (see Materials and Methods).

Long-term changes in temperature and salinity by region

Comparison of regional average differences in temperature and salinity between 1994 and 2016 for waters deeper than 2000 dbar reveals net warming and freshening over the last two decades in both the PET (64°S to 60°S) and the Australian-Antarctic Basin (60°S to 45°S) (Fig. 2, red and green curves, respectively). Below 2250 dbar, the regional-average warming signal is greater than 0.03°C in both regions (Fig. 2A). Significant freshening is also observed in both the Australian-Antarctic Basin and the PET (Fig. 2B). Average differences in temperature and salinity are accentuated in the abyss (P >3000 dbar) and are significant at well over the 95% confidence level (shading in the figure). The maximum basin-average warming and freshening signals in the Australian-Antarctic Basin are 0.13°C (0.06°C $decade^{-1}$) and 0.010 g/kg (0.005 g/kg $decade^{-1}$), respectively. The uncertainties on the mean differences are larger in the Australian-Antarctic Basin and in the PET than in the SAB because there are fewer effective degrees of freedom in these smaller regions (see Materials and Methods), and these isobaric coordinate averages include non-AABW waters. For example, in the Australian-Antarctic Basin at P > 3000 dbar, there is not only AABW but also the relatively saltier Lower Circumpolar Deep Water (LCDW, $28.18 < \gamma^n < 28.27$) (*16*).

Along I08S in the SAB (45°S to 30°S), no waters classifiable as AABW exist, although some freshening/warming signals are observed between 1994 and 2016 (Fig. 2, blue curves). Freshening is found between 2500 and 3500 dbar with a maximum of 0.003 g/kg (0.001 g/kg $decade^{-1}$). Slight warming is found below 3600 dbar, with a maximum of 0.04°C (0.02°C $decade^{-1}$) near the bottom. These results are not surprising because bottom waters of southern origin have taken longer to find their way into this more northerly basin, which is separated from those to the south by the fractured Southeast Indian Ridge system. Moreover, the I08S line in the SAB is not ideal for following the pathways of AABW (Fig. 1).

Spatiotemporal patterns of the AABW changes between 1994/2007 and 2016

Between 2007 and 2016, the meridional section of temperature changes in the AABW domain shows vertical bands of alternating positive and negative values (Fig. 3A). A previous study (*6*) that looked at the two

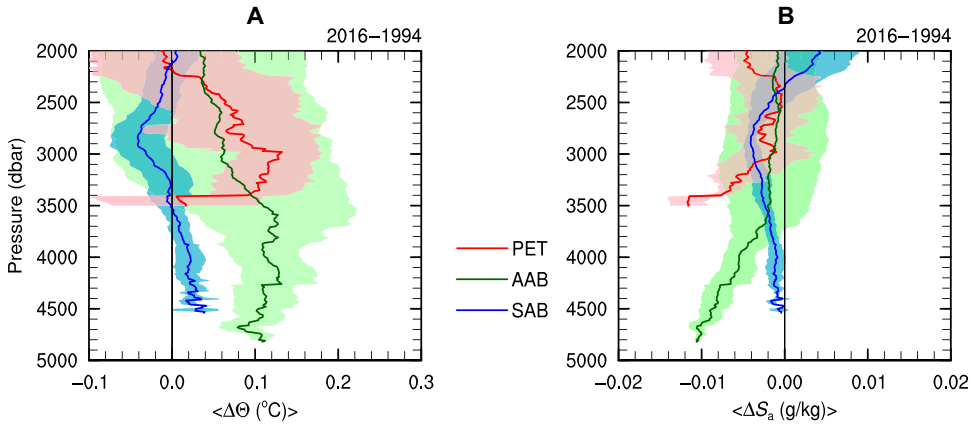

Fig. 2. Regional long-term changes in temperature and salinity. Mean differences in conservative temperature (ΔΘ) (**A**) and Absolute Salinity (ΔS_a) (**B**) between 1994 and 2016. Red curves represent the PET region (64°S to 60°S), green curves represent the Australian-Antarctic Basin (60°S to 45°S), and blue curves represent the SAB (45°S to 30°S). Shading indicates 95% confidence intervals (CIs) on the means.

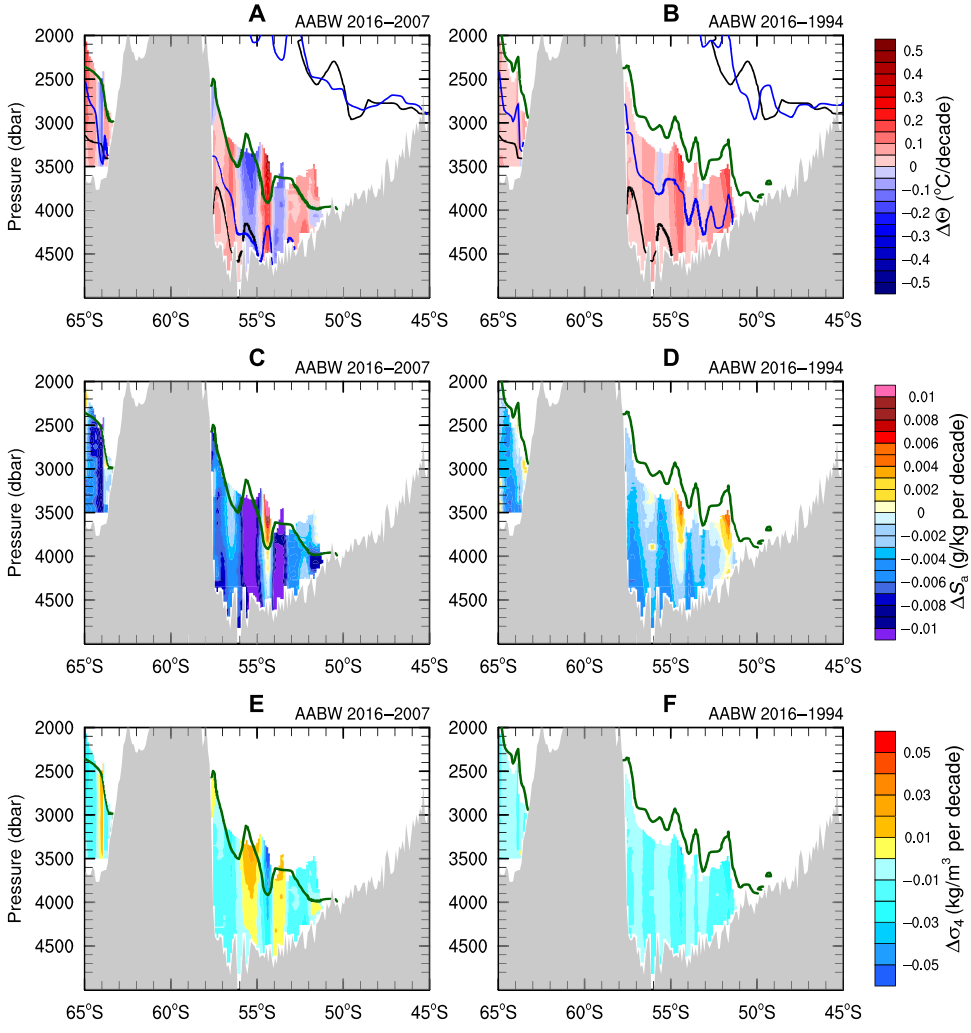

Fig. 3. Spatiotemporal patterns of the AABW rates of changes. Rates of change in conservative temperature (ΔΘ) (**A** and **B**), Absolute Salinity (ΔS_a) (**C** and **D**), and potential density referenced to 4000 dbar ($\Delta\sigma_4$) (**E** and **F**) in the AABW domain. Left and right columns show differences between 2007 to 2016 and 1994 to 2016, respectively. AABW domain is defined as the region where θ < 0°C in any I08S occupation. (A and B) Black curves are σ_4 = 45.9 and 46.1 kg/m^3 for 2016. Blue curves are the same isopycnals for 2007 in (A) and 1994 in (B). Thick green curves indicate γ^n = 28.27 kg/m^3 in 2016 (left plots) and 1994 (right plots). Gray shading indicates bottom topography.

earlier sections (1994 and 2007) suggested that this mesoscale banded pattern might be associated with eddies from the so-called Kerguelen Plateau Eddy Field (Fig. 1), internal waves and tides, or meridional shifts in currents and fronts in the region. This explanation holds for the most recent data set where the strongest cooling around 56°S to 55°S is, according to altimetry, associated with a cold core eddy present in 2016, but not in 2007 (fig. S1). The 2016 cold core eddy has a strong signature from the ocean surface to the bottom, which is represented by a vertical uplift of isopycnals (solid curves in Fig. 3A) and isotherms (fig. S1C). In contrast, a warm core eddy occupied this same region in 2007 (fig. S1B), deepening the isotherms (fig. S1D).

Mesoscale features aside, a substantial portion of AABW warmed from 2007 to 2016, as shown in the histogram of temperature changes that includes only AABW data from the PET and the Australian-Antarctic Basin (Fig. 4). The mean AABW warming is small (0.02° ± 0.03°C), but a large portion of the AABW (57%) is warmer than the mean. The warming from 2007 to 2016 is clear whether we compare the mean temperature or the temperature envelopes of AABW (see table S2 where the mean temperature and salinity of the AABW and the respective envelopes are calculated using both $\theta < 0$°C and $\gamma^n > 28.27$ kg/m^3 criteria for each occupation individually).

The banded pattern of positive/negative values described above for decadal differences is still present when changes are calculated between 1994 and 2016, but the regional warming amplitude is larger than the mesoscale signal. Over this 22-year period, an unequivocal warming of the abyssal waters in the PET and in the Australian-Antarctic Basin is observed (Fig. 3B). Maximum AABW temperature differences reach as high as 0.49°C over 22 years (0.22°C decade^{-1}). The mean AABW rate of temperature change estimated from the histogram in Fig. 4B is 0.06° ± 0.01°C decade^{-1}, with 85% of the data warming by more than 0.02°C decade^{-1} (the mean 2016–2007 rate of change). Throughout this paper, the word "data" refers to the AABW domain.

The warming of abyssal waters is accompanied by changes in salinity, with a clear freshening signal of up to 0.015 g/kg between 1994 and 2016 (Fig. 3, C and D). Much of the AABW domain has become fresher whether we compare 2016 to 2007 (92% of the data) or 2016 to 1994 (81%) (Fig. 4, C and D). The mean rates of change in salinity are about −0.006 ± 0.002 g/kg decade^{-1} and −0.002 ± 0.001 g/kg decade^{-1}, respectively. This freshening signal is expressed as a continuing decrease in both the mean and the maximum salinity of AABW in each of the two I08S reoccupations since 1994 (table S2). As with the temperature section, there is a banding in the pattern of salinity change. In the 22-year comparison, strong freshening in the deep abyss is particularly evident (Fig. 3D).

The observed warming and freshening signals reduce the density of the abyssal waters, making AABW lighter by about 0.025 kg/m^3 (0.011 ± 0.002 kg/m^3 decade^{-1}) in both the PET and the Australian-Antarctic Basin (Fig. 3, E and F). The densest Australian-Antarctic Basin isopycnals seen in 1994 ($\gamma^n = 28.345$ kg/m^3) are not found in 2007, and the same is true comparing 2007 (maximum $\gamma^n = 28.340$ kg/m^3) to 2016 (maximum $\gamma^n = 28.324$ kg/m^3), indicating a decline in the densest variety of AABW in this basin (table S2). A similar decline is evident in the PET. Furthermore, the $\sigma_4 = 46.10$ kg/m^3 or $\gamma^n = 28.31$ kg/m^3 isopycnals that lay in the core of the AABW in 1994 (blue curves in Fig. 3B) have deepened by more than 600 dbar in two decades and are found close to the bottom in the 2016 occupation (black curve in the same figure).

Abyssal changes in density space

Analysis of salinity and temperature variations in density space supports the pressure space analysis that show that waters denser than

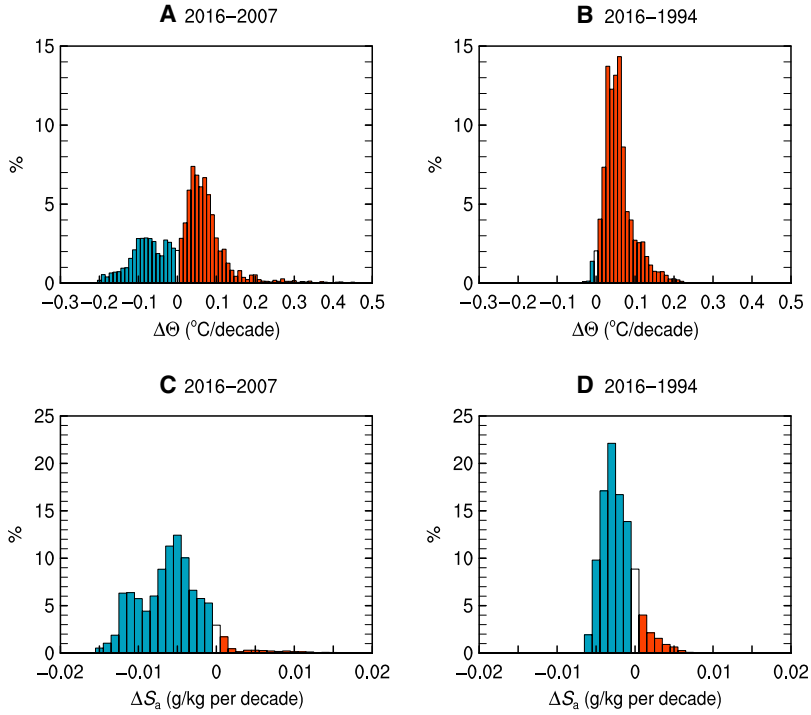

Fig. 4. AABW changes north of 64°S. Histograms of AABW changes north of 64°S (includes both the PET and the Australian-Antarctic Basin) for conservative temperature ($\Delta\Theta$) and Absolute Salinity (ΔS_a) between 2007 and 2016 (**A** and **C**) and 1994 and 2016 (**B** and **D**). Blue indicates negative changes (cooling/freshening), red indicates positive changes (warming/salinification), and white indicates small/zero change. The *y* axis shows the percentage of grid cells that fall into each interval (bin) (*x* axis) normalized by the total number classified as AABW ($\theta < 0$°C).

28.0 kg/m^3 (γ^n) have become colder and fresher since 1994. In these waters, the freshening and cooling signals are observed all the way along the I08S line, but the freshening is particularly enhanced (> 0.01 g/kg) in the AABW domain of the PET and the Australian-Antarctic Basin between 2007 and 2016 (fig. S2). By definition, freshening on density space must be associated with cooling.

Australian-Antarctic Basin: Θ-*S* and steric height changes (1994–2007 versus 2007–2016)

The observations from the I08S reoccupations in 1994, 2007, and 2016 suggest that the relationship between temperature and salinity in the abyssal waters of the Australian-Antarctic Basin has changed over the course of the last two decades. From 1994 to 2016, there is a consistent shift of the mean Θ-*S* curves toward lower salinities over much of the deep water column. This shift is enhanced in AABW (gray shading in Fig. 5), where, as mentioned earlier, the salinity differences reach 0.015 g/kg between 1994 and 2016. However, note that the 1994 and 2007 curves are closer to one another than to the 2016 curve, indicating that the changes in temperature and salinity were not the same in earlier and later decades. The first decade (2007–1994) is characterized by a strong warming of abyssal waters and a moderate freshening. The mean AABW warming in the Australian-Antarctic Basin is 0.08° ± 0.03°C decade^{-1}, with 84% of the data showing rates of change greater than 0.02°C decade^{-1} (Fig. 6A). This warming signal is of the same order as previously described by Johnson *et al.* (*6*) (warming of 0.1°C). Only 40% of the data classified as AABW show decreasing salinity in this period (Fig. 6B). In contrast, the second decade (2016–2007) is characterized by a strong freshening (93% of the data) and a moderate warming. About 57% of the data show a warming signal greater than the mean value (0.02° ± 0.02°C decade^{-1}) (Fig. 6A, shading). Clear shifts in the statistical distributions of both temperature and salinity changes exist (Fig. 6, A and B). The distributions are displaced toward lower temperatures and salinities in the second decade, which indicates a slowing of the warming and an acceleration of the freshening signal.

The differences between the freshening rates are particularly evident when analyzed in density space (Fig. 6C). In the first decade, the maximum freshening signal is 0.004 ± 0.001 g/kg decade^{-1} at γ^n = 28.32, and the mean is 0.002 ± 0.001 g/kg decade^{-1}. In the second decade, the minimum estimated freshening is much greater, 0.006 ± 0.001 g/kg decade^{-1} (γ^n = 28.23), and the maximum reaches 0.011 ± 0.001 g/kg decade^{-1} at γ^n = 28.32, with a mean value of 0.008 ± 0.001 g/kg decade^{-1}. LCDW (28.18 < γ^n < 28.27) has also freshened in the Australian-Antarctic Basin in the last decade.

In the Australian-Antarctic Basin, the temperature and salinity changes in the abyssal water result in a 2- to 3-cm decade^{-1} increase in steric height between 1994 and 2016, especially below 4000 dbar (fig. S3A). This long-term steric height variation is controlled by the temperature (warming) change (>85%), which predominantly occurred in the first decade (2007–1994) (Fig. 6A). Here, only below 4300 dbar does salinity contribute to steric height changes. In the second decade (2016–2007), the rate of change in steric height attributed to abyssal changes is reduced to about 1 cm decade^{-1} and is not significantly different from zero (fig. S3B). This local deceleration of steric sea level rise is connected to the slowdown in AABW warming over the last decade.

Comparing data from the 1994 and 2007 occupations, Johnson *et al.* (*6*) estimated a similar steric sea level rise of 1 to 4 cm in the Australian-Antarctic Basin. Our results suggest that the variation between 2007 and 2016 contributed less to sea level rise observed over the last 22 years than the changes from the first decade. Basin-average estimates of the contribution of abyssal warming to the sea level rise in the southeastern Indian Ocean are about 0.32 ± 0.017 cm decade^{-1} (*8*) and 0.25 ± 0.17 cm decade^{-1} (*10*), which would result in a sea level increase of 0.7 ± 0.4 cm (0.5± 0.4 cm) over 22 years. These estimates are lower than the increase suggested by I08S data reported by Johnson *et al.* (*6*) and confirmed here. However, this is not unexpected, because the estimates by Purkey

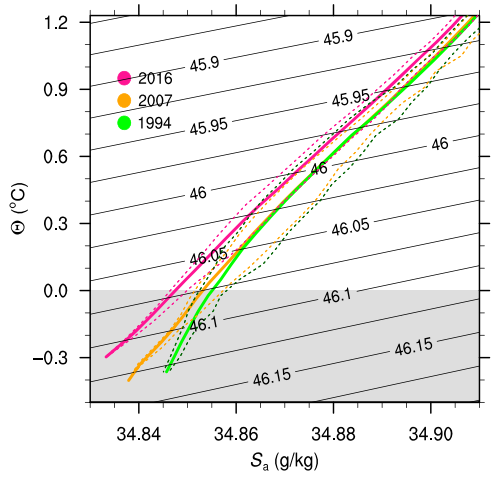

Fig. 5. Conservative temperature–Absolute Salinity (Θ – S_a) relationships in 1994 (green), 2007 (orange), and 2016 (pink) in the Australian-Antarctic Basin (60°S to 45°S). Colored solid curves indicate means computed on isopycnals, and dashes are the respective minima and maxima. Black curves are σ_4 densities. Gray shading indicates Θ < 0°C (AABW region).

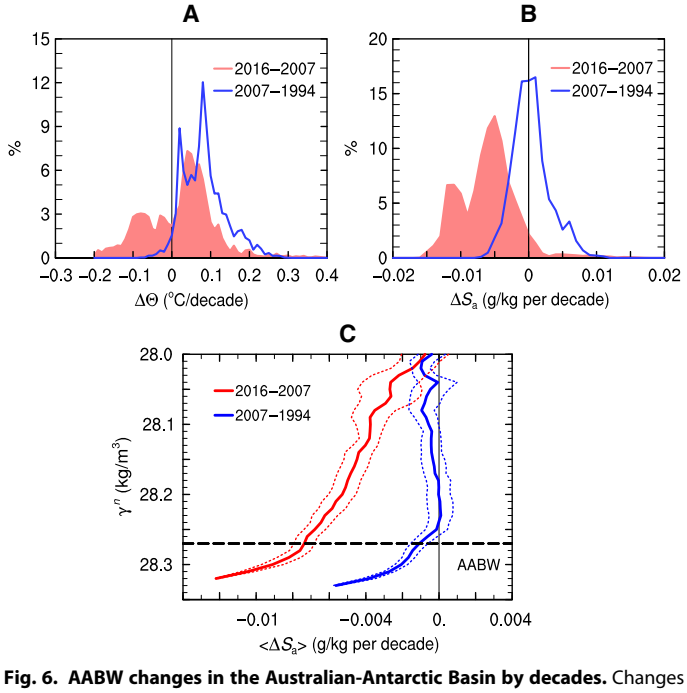

Fig. 6. AABW changes in the Australian-Antarctic Basin by decades. Changes in conservative temperature (ΔΘ) (**A**) and Absolute Salinity (ΔS_a) (**B**) for the AABW in the Australian-Antarctic Basin (60°S to 45°S). Reddish shadings are used for the differences between 2007 and 2016, and blue curves are used for differences between 1994 and 2007. Vertical black lines mark zero change. (**C**) Changes in Absolute Salinity between 2007 and 2016 and between 1994 and 2007 averaged (density space) over the Australian-Antarctic Basin. Dashed curves are 95% CIs on the means.

and Johnson (*8*, *10*) are averaged over a broader region and therefore likely include both younger and older bottom waters.

DISCUSSION

The freshening, warming, and resulting decreasing density of AABW from the 1990s through the early 2000s have previously been described by several studies and are now well documented in the literature especially in the Indo-Pacific region (*2*–*14*). Here, we introduce new evidence indicating that abyssal waters in the Australian-Antarctic Basin and the PET continue to become fresher, warmer, and less dense, although not at the same pace.

The high-quality, multidecadal hydrographic data used here were obtained in the same season and at approximately the same location (except in the far south, PET), mitigating possible temporal and spatial aliasing in the comparison of hydrographic snapshots (*4*, *5*, *12*). Although compared to 2007 the conductivity-temperature-depth (CTD) stations in the PET in 2016 were displaced westward by 2° to 7° because of ice cover and slightly eastward in 1994 (Fig. 1), the temporal changes observed in temperature and salinity in this region are consistent with the changes observed in the Australian-Antarctic Basin. Nevertheless, only values north of 64°S (where the I08S sections overlap) were used to estimate the basin averages and AABW differences presented here.

In contrast to the Australian-Antarctic Basin, the abyssal waters of the SAB did not change much, although a regional-average warming of about 0.04°C (0.02°C decade^{-1}) was detected near the bottom. The small variability in the abyssal waters of the SAB has previously been reported (*6*, *9*) and may be related to the quasi-zonal Southeast Indian Ridge (40°S to 50°S, depths < 3500 m) acting as a barrier to bottom waters, slowing down the northward progression of the signal.

This study found that AABW temperature and salinity changes during the 2007 to 2016 and 1994 to 2007 periods were not the same. In particular, between 2007 and 2016, AABW exhibited strong freshening (average of 0.008 ± 0.001 kg/g decade^{-1}) and only a slight warming in the Australian-Antarctic Basin. These changes have resulted in a continuing shift in the mean Θ-*S* curves toward lower densities. The shape of abyssal water Θ-*S* curves has also changed. In 1994, the tail of the Θ-*S* curve tends toward relatively higher salinities, whereas in 2007 and 2016, the tails have straightened, reflecting an increase in the strength of the freshening of the very bottom waters compared to the freshening of those just above.

Recent works (*9*, *11*, *12*) have suggested various underlying causes for the freshening and warming of AABW. There are two main possible causes that are not mutually exclusive (*12*). The first possibility is changes in the formation rate of the source waters; the second is a shift toward the formation of less dense bottom waters. It has been suggested (*9*) that AABW formation rates have decreased in all source regions around Antarctica, and the decline may have started as early as the 1950s. However, dissolved oxygen concentration variability along the pathway of the AABW to the Australian-Antarctic Basin is consistent with continued ventilation of AABW in the Indo-Pacific region over the last four decades (1970–2012) (*12*). Furthermore, chlorofluorocarbon (CFC) observations do not seem to indicate a strong change in AABW formation rate in this region (*12*).

There are several observations showing that dense Antarctic shelf waters, precursors of the AABW, are becoming fresher (0.003 decade^{-1}) both in the Ross Sea and along the George V/Adélie Land Coast (*2*, *4*, *7*, *29*). These results suggest that changes in the source waters, rather than formation rates, are the most likely causes of the freshening of the AABW in the Australian-Antarctic Basin (*12*). Because there is little change in source water temperature, the warming of the AABW in this basin is conjectured to be an indirect effect of the freshening through a combination of isopycnal and isotherm deepening (that is, heave), change in stratification, and enhanced vertical mixing (*11*, *12*).

If it is assumed that the observed changes of the AABW downstream in the Australian-Antarctic Basin reflect changes in the formation region, as suggested by the above-cited works, the question then becomes: What happened in the George V/Adélie Land region or the Ross Sea that may explain the accelerated freshening observed between 2007 and 2016?

In January to February 2010, an abrupt change occurred in the George V/Adélie Land region, with the calving of the Mertz Glacier Tongue (MGT), which resulted from the ungrounding of the large B9B iceberg (*30*–*32*). The coastal polynya regime over the Adélie Depression and Mertz Depression located west and east of the MGT is a key region for AABW formation (*25*). The dramatic MGT calving event and the repositioning of the B9B iceberg strongly reduced the salinity of dense shelf waters by more than 0.15 between 2008 and 2012 (*30*). It decreased sea ice production by 14 to 20% (*31*) and had the potential to decrease the export of dense shelf waters by more than 23% (*32*). Numerical simulations (*32*) showed that although shelf water became less dense due to the meltwater input, the exported shelf water from the Adélie Depression was still sufficiently dense to form AABW. This strong freshening after the MGT calving/B9B event is equivalent to 50 years of freshening at the long-term rate observed in the Ross Sea (*30*).

We conjecture that the strong decrease in AABW salinity in the Australian-Antarctic Basin observed between 2007 and 2016 may be linked to the MGT calving/B9B event that occurred in 2010. Previous work (*32*) has already speculated that this event could potentially impact AABW over a decadal time scale, because its effects may propagate through Kelvin and Rossby waves. Unfortunately, the transit time of AABW from the formation regions to the Australian-Antarctic Basin is not known. A back-of-envelope calculation, distance over time since the event (6 years), suggests that the magnitude of the mean abyssal currents would need to be on the order of 2 cm/s for the freshening signal from the MGT calving/B9B event to arrive at the Australian-Antarctic Basin through advection alone. Here, distance was defined as that following the schematic circulation shown in Fig. 1 between the Adélie Land Coast (146°E; 67°S) and 85°E; 66°S, plus the distance from this position to the Australian-Antarctic Basin (57°S; 82°E). This mean speed is plausible because there is a vigorous system of boundary currents transporting AABW westward at this latitude (*16*). East of the Kerguelen plateau near 57°S, observed mean speeds over 2 years exceed 20 cm/s at depths of about 3500 m (*27*). Analysis of CFCs from the 2007 occupation of I08S suggests that the apparent AABW mean age in the Australian-Antarctic Basin is about 40 years, but a substantial fraction is probably younger than this (time scales of a few decades or less) (*6*). Whether the strong freshening of the AABW in the Australian-Antarctic Basin reported here is a result of this particular event is still to be investigated and will require further effort by both the observational and modeling communities.

MATERIALS AND METHODS

Data

For this investigation, temperature and salinity observations collected by CTD sensors from three repeat occupations of the I08S (95°E)

hydrographic transect were used (Fig. 1). The cruises took place during the austral summers of 2016 (February to March, GO-SHIP), 2007 [February to March, Climate Variability and Predictability (CLIVAR)] and 1994 [December, World Ocean Circulation Experiment (WOCE)]. Along these lines, the CTD stations were nominally 55 km (30 nautical miles) apart with closer station spacing across strong current and bathymetric features. Because of shifting ice patterns, the cruises did not follow the same track south of 63°S (Fig. 1). The most recent data set was displaced westward (by 2° to 7°) relative to the 2007 section. The southernmost limit of the 1994 I08S section was 63.25°S. Therefore, to make the comparison possible, these WOCE data were augmented by observations collected during the Australian WOCE SR03C cruise (stations 76 to 88; 26 to 28 January 1994). This same augmentation was used by Johnson *et al.* (*6*). The SR03C stations were displaced slightly east of the 2007 line (Fig. 1). See table S1 for details about the above-cited cruises.

The raw CTD data from the I08S sections were processed by the Scripps Oceanographic Data Facility and are publicly available at the CLIVAR Carbon Hydrographic Data Office (CCHDO) website. The processing includes the calibration of practical salinity (S_p) against in situ samples from Niskin bottles (up to 36) (*33*). In situ salinities were measured by Guildline 8400 Austosal salinometers calibrated using International Association for the Physical Sciences of the Oceans (IAPSO) Standard Sea Waters (SSW). Target accuracies for the GO-SHIP/CLIVAR/WOCE CTD data are 3 dbar for pressure (*P*), 0.002°C for in situ temperature [International Temperature Scale 1990 (ITS-90)], and 0.002 g/kg for salinity on the Absolute Salinity scale (TEOS-10) (*33*). With few exceptions, the final CTD vertical profiles span the full water column from the sea surface to 10 to 15 m above the seafloor with a vertical resolution of 2 dbar.

The SR03C CTD data are also available through the CCHDO and include full water-column vertical profiles. Because of instrumental difficulties, the SR03C data are less accurate than the GO-SHIP/CLIVAR/WOCE CTD set. The expected accuracy is 0.02°C for subzero temperatures and 0.005 (PSS-78) for salinity (*6*, *34*).

Following the work of Johnson *et al.* (*6*) and of Purkey and Johnson (*10*), small offsets have been applied to the 1994 and 2007 I08S and 1994 SR03C practical salinity data to take into account the known IAPSO SSW batch-to-batch differences (*10*, *35*). No batch-to-batch offset has been applied to the 2016 I08S salinities because it is not available yet. These batch-to-batch offsets are in general very small, that is, on the order of the expected accuracy of the salinity measurements [see Table A1 of the study by Purkey and Johnson (*10*)] and are therefore of little quantitative consequence to our results. The offset for the 1994 I08S is 0.6×10^{-3}, for the 2007 I08S is -0.5×10^{-3}, and for the SR03C is 0.7/0.4×10^{-3} (more than one SSW batch was used). The ad hoc offsets proposed by Purkey and Johnson (*10*) to minimize the biases between cruises have also been applied to the (1994 and 2007) salinity data. Taking into account both corrections, the total offsets applied are -0.2×10^{-3} (1994 I08S), 0.302×10^{-3} (2007 I08S), 0.906×10^{-3} (1994 SR03C, stations 76 to 79), and 0.606×10^{-3} (1994 SR03C, stations 8 to 80), respectively (*10*). We also computed an ad hoc offset for the 2016 occupation by comparing salinity differences in the region of the I08S CFC minimum. Following the work by Purkey and Johnson (*10*), the 2016 CFC-12 data were mapped onto a 0.001°C-resolution isentropic grid. The lowest 2016 CFC concentrations (< 0.05 pmol/kg) were found in the SAB north of 36°S between 0.7° and 3.1°C. To be consistent with earlier analyses (*6*, *8*, *10*), an ad hoc offset of −0.001 has been applied to the 2016 data. These ad hoc salinity offsets are of the same order (usually less) of the salinity measurement accuracy (about 0.002).

Processing

The CTD data for this study were processed in fashion similar to that used by Johnson *et al.* (*6*) and Purkey and Johnson (*8*, *10*), except that here, the new equation of state of seawater TEOS-10 (*28*) was used. The in situ temperature (ITS-90) and adjusted salinity (PSS-78) were used to derive potential (θ) and conservative (Θ) temperatures, Absolute Salinity (S_a), potential density referenced to 4000 dbar (σ_4), and neutral density (γ^n) (*36*). Both densities were computed so that present results could be compared to those in the published literature (*5*, *6*, *12*, *37*). All the above quantities were derived using the Gibbs SeaWater Oceanographic Toolbox of TEOS-10 version 3.05 (*38*), except γ^n, which was estimated using Ocean Data View software (*39*).

Vertical profiles of the derived fields were smoothed with a 20-dbar half-width Hanning filter and linearly interpolated to a 10-dbar pressure grid. The smoothed data were then interpolated onto an evenly spaced latitudinal grid (0.1°) between 65°S and 30°S using a piecewise cubic Hermite polynomial. The 0.1° × 10-dbar grid resulted in a total number of observations that were similar to the original data sets. The Smith-Sandwell bathymetry (*40*) was used to eliminate data that had been interpolated below 20 m above the ocean floor. Extrapolation was avoided so that comparisons between the data sets did not include its effects. Analyses were carried out in both pressure and isopycnal (γ^n) vertical coordinates following the study by Johnson *et al.* (*6*). For the isopycnal coordinate analysis, the derived fields for P >2000 dbar are interpolated onto a finely spaced (0.01-kg/m^3) γ^n grid. Mean temperature-salinity relations were estimated on the isopycnal grid. Differences between the I08S sections were calculated by subtracting the earlier I08S data from the more recent data (for example, Δ = 2016–2007) in the gridded coordinate system.

To evaluate the impact of temperature and salinity on thermosteric sea level (*sl*), steric heights referenced to 3000 dbar (integrated from bottom to top) have been computed for each I08S occupation after the study by Johnson *et al.* (*6*). To resolve the relative individual contributions of temperature and salinity variations to the steric sea level variability, two additional estimates of steric height referenced to 3000 dbar were calculated. One of these estimates was based on temperature variations, and the other was based on salinity variations.

Average differences were computed for the PET, the Australian-Antarctic Basin, and the SAB. To mitigate possible spatial aliasing caused by the zonal displacement at the southern end of the I08S line in the various occupations, only data north of 64°S were used (see Fig. 1). Thus, the PET was defined here as the region between 64°S and 60°S instead of the 66°S to 60°S interval used by Johnson *et al.* (*6*).

For the regional average differences, the 95% CIs for the mean were estimated using a similar approach to that used by Johnson *et al.* (*6*) and Purkey and Johnson (*8*). The CI is estimated assuming a Student's t distribution and is given by $\bar{x} \pm t_{\alpha/2,N^*-1} \frac{s}{\sqrt{N^*}}$, where $\bar{x}$ is the sample mean, $t_{\alpha/2,N^*-1}$ is the Student's t multiplier, which depends on the significance level (α) and degrees of freedom, and s is the sample standard deviation. Here, N^* is the effective degrees of freedom (*41*). A similar definition of N^* as in the study by Purkey and Johnson (*8*) was used, such that N^* at each pressure/isopycnal level was given by the latitudinal length of the basin divided by a single spatial decorrelation scale of 160 km.

To estimate the average differences for AABW, only the grid points (pressure, latitude) classifiable as AABW were selected (θ < 0°C). These data were used to construct histograms for the AABW differences in temperature and salinity. Mean values for AABW differences and respective 95% CI were then estimated using an empirical bootstrap method (*42*). The empirical bootstrap provides a direct computational

method for assessing statistical accuracy without assumptions about the underlying distribution. It is a resampling technique in which artificial bootstrap samples are drawn by random sampling of the training data. Here, we used the bias-corrected and accelerated bootstrap method with 1000 samples, which included adjustment for bias and skewness in the empirical distribution. We tested different sample sizes (100 to 10,000), with results being the same for sizes larger than 1000. Because our data were correlated in both the horizontal and vertical directions, a moving block bootstrap approach was used (*43*, *44*). Block bootstraps are commonly used to analyze autocorrelated data, such as those from geophysical time series. The main idea is to resample the observations in blocks instead of single elements to capture the dependences in autocorrelated data sets. There are several techniques to determine the optimal block lengths, but here, to maintain consistency with the Student's *t* analysis, the block length is defined as the horizontal decorrelation scale (160 km) times the thickness of the AABW layer.

SUPPLEMENTARY MATERIALS

Supplementary material for this article is available at http://advances.sciencemag.org/cgi/content/full/3/1/e1601426/DC1

table S1. Details about the I08S (95°E) occupations in the Indian sector of the Southern Ocean.

table S2. AABW mean conservative temperature, Absolute Salinity, and respective envelopes (minimum and maximum values) in 1994, 2007, and 2016 for the PET (64°S to 60°S) and the Australian-Antarctic Basin (60°S to 45°S).

fig. S1. Snapshots of the Australian-Antarctic Basin: Sea surface height anomaly and absolute geostrophic currents from multisatellite altimetry.

fig. S2. Rates of change in conservative temperature and Absolute Salinity in density space (neutral density).

fig. S3. Rates of change in steric height in the Australian-Antarctic Basin.

REFERENCES AND NOTES

1. N. L. Bindoff, W. R. Hobbs, Deep ocean freshening. *Nat. Clim. Chang.* **3**, 864–865 (2013).
2. T. Whitworth III, Two modes of bottom water in the Australian-Antartic basin. *Geophys. Res. Lett.* **29**, 17-1–17-3 (2002).
3. S. S. Jacobs, Bottom water production and its links with the thermohaline circulation. *Antarct. Sci.* **16**, 427–437 (2004).
4. S. Aoki, S. R. Rintoul, S. Ushio, S. Watanabe, N. L. Bindoff, Freshening of the Adélie Land Bottom Water near 140°E. *Geophys. Res. Lett.* **32**, L23601 (2005).
5. S. R. Rintoul, Rapid freshening of Antarctic Bottom Water formed in the Indian and Pacific oceans. *Geophys. Res. Lett.* **34**, L06606 (2007).
6. G. C. Johnson, S. G. Purkey, J. L. Bullister, Warming and freshening in the abyssal southeastern Indian Ocean. *J. Climate* **21**, 5351–5363 (2008).
7. S. S. Jacobs, C. F. Giulivi, Large multidecadal salinity trends near the Pacific-Antarctic continental margin. *J. Climate* **23**, 4508–4524 (2010).
8. S. G. Purkey, G. C. Johnson, Warming of global abyssal and deep Southern Ocean Waters between the 1990s and 2000s: Contributions to global heat and sea level rise budgets. *J. Climate* **23**, 6336–6351 (2010).
9. S. G. Purkey, G. C. Johnson, Global contraction of Antarctic Bottom Water between the 1980s and 2000s. *J. Climate* **25**, 5830–5844 (2012).
10. S. G. Purkey, G. C. Johnson, Antarctic Bottom Water warming and freshening: Contributions to sea level rise, ocean freshwater budgets, and global heat gain. *J. Climate* **26**, 6105–6122 (2013).
11. K. Shimada, S. Aoki, K. I. Ohshima, S. R. Rintoul, Influence of Ross Sea Bottom Water changes on the warming and freshening of the Antarctic Bottom Water in the Australian-Antarctic basin. *Ocean Sci.* **8**, 419–432 (2012).
12. E. M. van Wijk, S. R. Rintoul, Freshening drives contraction of Antarctic Bottom Water in the Australian Antarctic basin. *Geophys. Res. Lett.* **41**, 1657–1664 (2014).
13. L. Jullion, A. C. Naveira Garabato, M. P. Meredith, P. R. Holland, P. Courtois, B. A. King, Decadal freshening of the Antarctic Bottom Water exported from the Weddell Sea. *J. Climate* **26**, 8111–8125 (2013).
14. S. Aoki, Y. Kitade, K. Shimada, K. I. Ohshima, T. Tamura, C. C. Bajish, M. Moteki, S. R. Rintoul, Widespread freshening in the seasonal ice zone near 140e off the Adélie Land Coast, Antarctica, from 1994 to 2012. *J. Geophys. Res.* **118**, 6046–6063 (2013).
15. F. A. Haumann, N. Gruber, M. Münnich, I. Frenger, S. Kern, Sea-ice transport driving Southern Ocean salinity and its recent trends. *Nature* **537**, 89–92 (2016).
16. A. H. Orsi, G. C. Johnson, J. L. Bullister, Circulation, mixing, and production of Antarctic Bottom Water. *Progr. Oceanogr.* **43**, 55–109 (1999).
17. G. C. Johnson, Quantifying Antarctic Bottom Water and North Atlantic Deep Water volumes. *J. Geophys. Res.* **113**, C05027 (2008).
18. S. G. Purkey, G. C. Johnson, D. P. Chambers, Relative contributions of ocean mass and deep steric changes to sea level rise between 1993 and 2013. *J. Geophys. Res.* **119**, 7509–7522 (2014).
19. D. M. Sigman, M. P. Hain, G. H. Haug, The polar ocean and glacial cycles in atmospheric CO_2 concentration. *Nature* **466**, 47–55 (2010).
20. C. T. Hayes, A. Martínez-García, A. P. Hasenfratz, S. L. Jaccard, D. A. Hodell, D. M. Sigman, G. H. Haug, R. F. Anderson, A stagnation event in the deep South Atlantic during the last interglacial period. *Science* **346**, 1514–1517 (2014).
21. Z. Lu, B. A. A. Hoogakker, C.-D. Hillenbrand, X. Zhou, E. Thomas, K. M. Gutchess, W. Lu, L. Jones, R. E. M. Rickaby, Oxygen depletion recorded in upper waters of the glacial Southern Ocean. *Nat. Commun.* **7**, 11146 (2016).
22. K. I. Ohshima, Y. Fukamachi, G. D. Williams, S. Nihashi, F. Roquet, Y. Kitade, T. Tamura, D. Hirano, L. Herraiz-Borreguero, I. Field, M. Hindell, S. Aoki, M. Wakatsuchi, Antarctic Bottom Water production by intense sea-ice formation in the Cape Darnley polynya. *Nat. Geosci.* **6**, 235–240 (2013).
23. L. Talley, R. A. Feely, B. M. Sloyan, R. Wanninkhof, M. O. Baringer, J. L. Bullister, C. A. Carlson, S. C. Doney, R. A. Fine, E. Firing, N. Gruber, D. A. Hansell, M. Ishii, G. C. Johnson, K. Katsumata, R. M. Key, M. Kramp, C. Langdon, A. M. Macdonald, J. T. Mathis, E. L. McDonagh, S. Mecking, F. J. Millero, C. W. Mordy, T. Nakano, C. L. Sabine, W. M. Smethie, J. H. Swift, T. Tanhua, A. M. Thurnherr, M. J. Warner, J.-Z. Zhang, Changes in ocean heat, carbon content, and ventilation: A review of the first decade of GO-SHIP global repeat hydrography. *Ann. Rev. Mar. Sci.* **8**, 185–215 (2016).
24. A. W. Mantyla, J. L. Reid, On the origins of deep and bottom waters of the Indian Ocean. *J. Geophys. Res.* **100**, 2417–2439 (1995).
25. G. D. Williams, S. Aoki, S. S. Jacobs, S. R. Rintoul, T. Tamura, N. L. Bindoff, Antarctic Bottom Water from the Adélie and George V Land coast, East Antarctica (140–149°E). *J. Geophys. Res.* **115**, C04027 (2010).
26. S. Aoki, N. Fujii, S. Ushio, Y. Yoshikawa, S. Watanabe, G. Mizuta, Y. Fukamachi, M. Wakatsuchi, Deep western boundary current and southern frontal systems of the Antarctic Circumpolar Current southeast of the Kerguelen Plateau. *J. Geophys. Res.* **113**, C08038 2008).
27. Y. Fukamachi, S. R. Rintoul, J. A. Church, S. Aoki, S. Sokolov, M. A. Rosenberg, M. Wakatsuchi, Strong export of Antarctic Bottom Water east of the Kerguelen plateau. *Nat. Geosci.* **3**, 327–331 (2010).
28. Intergovernmental Oceanographic Commission, Scientific Committee on Oceanic Research, International Association for the Physical Sciences of the Oceans, *The International Thermodynamic Equation of Seawater—2010: Calculation and Use of Thermodynamic Properties*, Intergovernmental Oceanographic Commission, Manuals and Guides 56 (UNESCO, 2010).
29. S. S. Jacobs, C. F. Giulivi, P. A. Mele, Freshening of the Ross Sea during the late 20th century. *Science* **297**, 386–389 (2002).
30. E. H. Shadwick, S. R. Rintoul, B. Tilbrook, G. D. Williams, N. Young, A. D. Fraser, H. Marchant, J. Smith, T. Tamura, Glacier tongue calving reduced dense water formation and enhanced carbon uptake. *Geophys. Res. Lett.* **40**, 904–909 (2013).
31. T. Tamura, G. D. Williams, A. D. Fraser, K. I. Ohshima, Potential regime shift in decreased sea ice production after the Mertz Glacier calving. *Nat. Commun.* **3**, 826 (2012).
32. K. Kusahara, H. Hasumi, G. D. Williams, Impact of the Mertz Glacier Tongue calving on dense water formation and export. *Nat. Commun.* **2**, 159 (2011).
33. E. Hood, C. Sabine, B. M. Sloyan, Eds., "The GO-SHIP Repeat Hydrography manual: A collection of expert reports and guidelines" (Technical Report, IOCCP Report No. 14, ICPO Publication Series No. 134, International CLIVAR Project Office, 2010); www.go-ship.org/HydroMan.html [accessed 12 December 2016].
34. M. Rosenberg, R. Eriksen, S. Bell, N. Bindoff, S. Rintoul, "Aurora Australis marine science cruise au9407 - Oceanographic field measurements and analysis" (Technical Report, Antarctic CRC Research Report, 1995).
35. T. Kawano, M. Aoyama, T. Joyce, H. Uchida, Y. Takatsuki, M. Fukasawa, The latest batch-to-batch difference table of standard seawater and its application to the WOCE one time sections. *J. Oceanogr.* **62**, 777–792 (2006).
36. D. R. Jackett, T. J. McDougall, A neutral density variable for the world's oceans. *J. Phys. Oceanogr.* **27**, 237–263 (1997).
37. N. Anilkumar, R. Chacko, P. Sabu, J. V. George, Freshening of Antarctic Bottom Water in the Indian ocean sector of Southern ocean. *Deep Sea Res. Pt. II* **118**, 162–169 (2015).
38. T. J. McDougall, P. M. Barker, Getting started with TEOS-10 and the Gibbs Seawater (GSW) oceanographic toolbox (2011), SCOR/IAPSO WG127, ISBN 978-0-646-55621-5.
39. R. Schlitzer, "Ocean Data View" (Technical Report, 2015); http://odv.awi.de/en/home/. [accessed 12 December 2016].
40. W. H. F. Smith, D. T. Sandwell, Global seafloor topography from satellite altimetry and ship depth soundings. *Science* **277**, 1956–1962 (1997).

41. W. J. Emery, R. E. Thomson, *Data Analysis Methods in Physical Oceanography* (Elsevier, New York, 2001).
42. T. Hastie, R. Tibshirani, J. Friedman, *The Elements of Statistical Learning: Data Mining, Inference, and Predictions* (Springer Series in Statistics, Springer, New York, ed. 2, 2009).
43. D. S. Wilks, Resampling hypothesis tests for autocorrelated fields. *J. Climate* **10**, 65–82 (1997).
44. X. Feng, T. DelSole, P. Houser, Bootstrap estimated seasonal potential predictability of global temperature and precipitation. *Geophys. Res. Lett.* **38**, L07702 (2011).

Acknowledgments: We thank the crew and science party on board the R/V *Revelle* for their efforts in support of the 2016 repeat occupation of the I08S line as well as all those who have gone before making the decadal comparison possible. V.V.M. also acknowledges interesting discussions with M. Vianna. We thank the two anonymous reviewers for their constructive comments and suggestions. **Funding:** The 2016 I08S cruise and the analysis and science performed at sea, as well as the individual principal investigators were funded through multiple National Oceanic and Atmospheric Administration (NOAA) and NSF grants including NSF grant OCE-1437015. The research for this article was mainly completed at sea. For land-based work, V.V.M. relied on her postdoctoral funding through NSF grant OCE-1435665, and A.M.M. was supported in part by NSF grant OCE-1356630 and NOAA grant NA11OAR4310063. **Author contributions:** V.V.M. and A.M.M. conceived the research and designed the analyses. C.S. processed the raw data. V.V.M. made all the figures and wrote the manuscript with contributions from A.M.M. The manuscript was revised by A.M.M. **Competing interests:** A.M.M. is an unpaid member of the U.S. Global Ocean Carbon and Repeat Hydrography Program oversight committee, which organizes U.S. GO-SHIP long-line hydrographic cruises, which the paper data is sourced from. The other authors declare that they have no competing interests. **Data and materials availability:** Data used in this work are available through the CCHDO website http://cchdo.ucsd.edu. All data needed to evaluate the conclusions in the paper are present in the paper and/or the Supplementary Materials. Additional data related to this paper may be requested from the authors.

Submitted 23 June 2016
Accepted 8 December 2016
Published 25 January 2017
10.1126/sciadv.1601426

Citation: V. V. Menezes, A. M. Macdonald, C. Schatzman, Accelerated freshening of Antarctic Bottom Water over the last decade in the Southern Indian Ocean. *Sci. Adv.* **3**, e1601426 (2017).

Accelerated freshening of Antarctic Bottom Water over the last decade in the Southern Indian Ocean

Viviane V. Menezes, Alison M. Macdonald and Courtney Schatzman

Sci Adv **3** (1), e1601426.
DOI: 10.1126/sciadv.1601426